

# On the Fragility of Nb-Ni Based and $\text{Zr}_{55-x}\text{Ti}_x(\text{CuNi})_{18.25+y}\text{Be}_{26.25-y}$ Bulk Metallic Glasses

Ludi A. Shadowspeaker and Ralf Busch

Department of Mechanical Engineering, Oregon State University, Corvallis Oregon 97331

## ABSTRACT

The heating rate dependencies of the glass transition temperature of the  $\text{Ni}_{65}\text{Nb}_{35}$ ,  $\text{Ni}_{60}\text{Nb}_{35}\text{Sn}_5$ ,  $\text{Ni}_{59.35}\text{Nb}_{34.45}\text{Sn}_{6.2}$ ,  $\text{Ni}_{60}(\text{Nb}_{40}\text{Ta}_{60})_{34}\text{Sn}_6$ , and  $\text{Ni}_{57}\text{Fe}_3\text{Nb}_{35}\text{Sn}_5$  metallic glass forming alloys were investigated with a differential scanning calorimeter (DSC). The relaxation time for each DSC experiment was plotted versus inverse temperature and a Vogel-Fulcher-Tamman (VFT) type relation was fit to the data. The fragilities of the alloys were characterized with the fragility parameter,  $D^*$ , and the VFT temperature,  $T_0$ , which are the fit parameters from the VFT relation. It was found that for the binary alloy  $D^* = 6.2$ , for the ternary alloys  $D^* = 11.0$ , and that for the quaternary alloys  $D^*$  was between 16.4 and 19.0, from which it was observed that  $D^*$  increased monotonically as the number of components in the alloy increased. This trend is also seen in Zr based alloys.

## INTRODUCTION

Novel multicomponent systems of glass forming alloys, such as La-Al-Ni [1], Zr-Ti-Cu-Ni [2], Zr-Ti-Cu-Ni-Be [3], and Zr-Ni-Al-Cu [4], exhibit very good glass forming ability. These bulk metallic glasses (BMG) show high thermal stability in their undercooled liquid state with respect to crystallization. It has been suggested that BMG forming liquids are rather strong liquids in the framework of the fragility concept [5]. This concept is a classification scheme to describe the different temperature dependencies of viscosity. For example, it has been shown for Zr-Ti-Cu-Ni-Be alloys [6] that their melt viscosities are about four orders of magnitude larger than those of pure metals. The temperature dependence of the viscosity can be described by a Vogel-Fulcher-Tamman (VFT) type relation [7]. Assuming Maxwell relaxation, the structural ( $\alpha$ -) relaxation time,  $\tau$ , of an alloy is proportional to its viscosity. Therefore  $\tau$  can also be described by a VFT type relation, and compared in the context of the fragility concept. This temperature dependence of  $\tau$  can be determined by measuring the heating rate dependence of the glass transition temperature [7,8]. Fragility (Angell) plots are a convenient way to compare the measured viscosities or relaxation times of different glass forming systems. This study focuses on the  $\text{Ni}_{65}\text{Nb}_{35}$ ,  $\text{Ni}_{60}\text{Nb}_{35}\text{Sn}_5$ ,  $\text{Ni}_{59.35}\text{Nb}_{34.45}\text{Sn}_{6.2}$ ,  $\text{Ni}_{60}(\text{Nb}_{40}\text{Ta}_{60})_{34}\text{Sn}_6$ , and  $\text{Ni}_{57}\text{Fe}_3\text{Nb}_{35}\text{Sn}_5$  glass forming alloys. The goal of this investigation is to describe how the fragilities of the Nb-Ni based alloys change with the addition of components to the system, and to compare the data with the previously determined fragilities of other alloys.

## EXPERIMENTAL METHODS

Master alloys of  $\text{Ni}_{65}\text{Nb}_{35}$ ,  $\text{Ni}_{60}\text{Nb}_{35}\text{Sn}_5$ ,  $\text{Ni}_{59.35}\text{Nb}_{34.45}\text{Sn}_{6.2}$ ,  $\text{Ni}_{60}(\text{Nb}_{40}\text{Ta}_{60})_{34}\text{Sn}_6$ , and  $\text{Ni}_{57}\text{Fe}_3\text{Nb}_{35}\text{Sn}_5$  were prepared by arc melting a mixture of the elements with a purity of 99.7 at% or better on a water-cooled copper boat under a Ti-gettered argon atmosphere. To obtain

glassy  $\text{Ni}_{60}\text{Nb}_{35}\text{Sn}_5$ ,  $\text{Ni}_{59.35}\text{Nb}_{34.45}\text{Sn}_{6.2}$ ,  $\text{Ni}_{60}(\text{Nb}_{40}\text{Ta}_{60})_{34}\text{Sn}_6$ , and  $\text{Ni}_{57}\text{Fe}_3\text{Nb}_{35}\text{Sn}_5$ , the alloys were remelted under vacuum in a quartz tube using an radio frequency induction coil and subsequently injection cast with argon into a copper mold. Amorphous  $\text{Ni}_{65}\text{Nb}_{35}$  ribbons were prepared by rapid quench in a melt spinner. The  $\text{Ni}_{60}\text{Nb}_{35}\text{Sn}_5$ ,  $\text{Ni}_{59.35}\text{Nb}_{34.45}\text{Sn}_{6.2}$ ,  $\text{Ni}_{60}(\text{Nb}_{40}\text{Ta}_{60})_{34}\text{Sn}_6$ , and  $\text{Ni}_{57}\text{Fe}_3\text{Nb}_{35}\text{Sn}_5$  samples were cut with a Buehler Isomet 1000 precision saw. Samples of  $\text{Ni}_{65}\text{Nb}_{35}$  were cut by hand from the melt-spun ribbons. Differential scanning calorimetric (DSC) measurements were performed on all the alloys using a Perkin-Elmer Pyris 1 DSC. The glass transition temperature,  $T_g$ , can be defined as the onset temperature of the endothermic DSC event, and the crystallization temperature,  $T_x$ , is defined as the onset temperature of the first exothermic DSC event. Both  $T_g$  and  $T_x$  depend on the heating rate. Samples were analyzed in the DSC between 573 K and 1023 K at heating rates between  $0.0167 \text{ K s}^{-1}$  and  $3.33 \text{ K s}^{-1}$ . The results of these experiments are summarized in Fig. 1 and Table I.

## RESULTS

In Fig. 1,  $T_g$  and  $T_x$  for the  $\text{Ni}_{65}\text{Nb}_{35}$  and  $\text{Ni}_{60}\text{Nb}_{35}\text{Sn}_5$  alloys are plotted versus the heating rate of the DSC. Table I summarizes the same results from the other alloys. Figure 1 shows that the effect of changing heating rate on  $T_g$  is small for the binary  $\text{Ni}_{65}\text{Nb}_{35}$  alloy, and larger for the ternary  $\text{Ni}_{60}\text{Nb}_{35}\text{Sn}_5$  alloy. The heating rate dependence of  $T_g$  is most pronounced for the quaternary  $\text{Ni}_{60}(\text{Nb}_{40}\text{Ta}_{60})_{34}\text{Sn}_6$  alloy. It is also interesting to note the heating rate dependence of the supercooled liquid region,  $\Delta T$ , which is the temperature range between  $T_g$  and  $T_x$ . It can be seen in Fig. 1 that  $\Delta T$  is smallest for the binary alloy and larger for the ternary alloy. For the binary alloy,  $\Delta T$  even vanishes for heating rates that are smaller than  $0.2 \text{ K s}^{-1}$ , because the alloy crystallizes before it undergoes the glass transition.  $\Delta T$  is the largest for the quaternary  $\text{Ni}_{60}(\text{Nb}_{40}\text{Ta}_{60})_{34}\text{Sn}_6$  alloy. From the DSC experiments it was possible to deduce the temperature dependence of the structural ( $\alpha$ -) relaxation time,  $\tau$ .

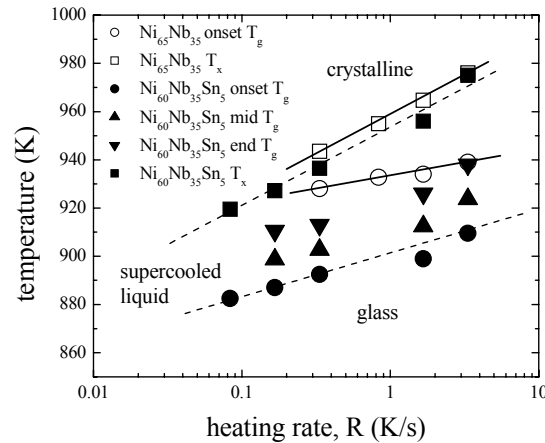


**Figure 1:** Onset glass transition temperature,  $T_g$ , and onset crystallization temperature,  $T_x$ , of binary  $\text{Ni}_{65}\text{Nb}_{35}$  and ternary  $\text{Ni}_{60}\text{Nb}_{35}\text{Sn}_5$  alloys plotted versus the heating rate,  $R$ , of the DSC.

**Table I:** Onset glass transition temperature,  $T_g$ , and crystallization temperature,  $T_x$ , at different heating rates shown for the three alloys studied that are not included in Fig. 1. The fragility parameters of these alloys are also shown.

R (Ks <sup>-1</sup> )	$T_g$ (K) Ni <sub>59.35</sub> Nb <sub>34.45</sub> Sn <sub>6.2</sub>	$T_x$ (K)	$T_g$ (K) Ni <sub>60</sub> (Nb <sub>40</sub> Ta <sub>60</sub> ) <sub>34</sub> Sn <sub>6</sub>	$T_x$ (K)	$T_g$ (K) Ni <sub>57</sub> Fe <sub>3</sub> Nb <sub>35</sub> Sn <sub>5</sub>	$T_x$ (K)
0.033	881	908			864	888.1
0.083	881.5	919.5	901.5	957.8	871	898.5
0.167	887	924.75	906.5	967.5	876	904.2
0.333	888.25	934.5				
0.833			921	987	890	922
1.667	904	960	928		897	932
3.333	905	967	941		905	948.1
D*	11.0		19.0		16.4	

Structural relaxation can be calorimetrically observed in the temperature interval,  $\Delta T_g$ , [7] which is defined as the temperature range between the onset and the end of the endothermic DSC event that is associated with the glass transition. At a constant heating rate, the average relaxation time,  $\tau$ , can be described as

$$\tau = \Delta T_g / R \quad (1)$$

where R is the heating rate in the DSC [7]. The  $T_g$  at a particular heating rate is used to approximate the temperature that corresponds to  $\tau$ . The temperature dependence of  $\tau$  can be described by the VFT type relation [8]

$$\tau = \tau_0 \exp\left(\frac{D^* \cdot T_0}{T - T_0}\right) \quad (2)$$

where  $D^*$  is the fragility parameter and  $T_0$  is the VFT temperature, which is defined as the temperature at which the relaxation time and thus the kinetic resistance to flow approaches infinity.  $D^*$  and  $T_0$  are used to quantify the fragility of the undercooled liquid. The strongest glass former SiO<sub>2</sub> has a fragility parameter of  $D^* \approx 100$ . The most fragile glass formers, such as pure metals, have a fragility parameter  $D^* \approx 2$ . Intermediate glass formers have a range of  $D^*$  from about 10 to 50.  $D^*$  and  $T_0$  are not independent parameters. Materials with higher values of  $D^*$  have smaller values for  $T_0$ .  $D^*$  and  $T_0$  are found by fitting the data to a VFT type relation.

To determine the fragility parameters in this investigation the relaxation times were determined with Eq. 1. These data were fitted with Eq. 2 using  $D^*$  and  $T_0$  as fit parameters.  $\tau_0$  is the value of the relaxation time in the limit as  $1/T \rightarrow 0$ . It has been shown that for all materials this time is very similar. The preexponential factor,  $\tau_0$ , only depends on the molar volume with  $\tau_0 \propto N_A \cdot h / V$ , where  $N_A$  is Avagadro's constant,  $h$  is Planck's constant and  $V$  is the molar volume [9]. Since the molar volume of these alloys is very similar,  $\tau_0$  was kept constant at  $2.5 \cdot 10^{-13}$  s in the VFT fits. This approximates the relaxation time for these alloys at infinite temperature.  $\Delta T_g$  was held constant at 25 K, which is a close approximation for  $\Delta T_g$  at all of the heating rates. The best fits of the data show the trend that  $D^*$  increases and  $T_0$  decreases with increasing complexity of the alloy. We find for the binary Ni<sub>65</sub>Nb<sub>35</sub> alloy  $D^* = 6.2$  and  $T_0 = 784$  K, for the ternary Ni<sub>60</sub>Nb<sub>35</sub>Sn<sub>5</sub> and Ni<sub>59.35</sub>Nb<sub>34.45</sub>Sn<sub>6.2</sub> alloys  $D^* = 11.0$  and  $T_0 = 670$  K, for the quaternary Ni<sub>57</sub>Fe<sub>3</sub>Nb<sub>35</sub>Sn<sub>5</sub> alloy  $D^* = 16.4$  and  $T_0 = 591$  K, and for the quaternary

$\text{Ni}_{60}(\text{Nb}_{40}\text{Ta}_{60})_{34}\text{Sn}_6$  alloy  $D^* = 19.0$ , and  $T_0 = 581$  K.  $D^*$  is shown for each alloy in Table I. These results can be compared on a fragility plot.

## DISCUSSION

The fragility plot for the Nb-Ni based alloys is shown in Fig. 2. In this plot the relaxation time is shown as a function of inverse temperature standardized by  $T_g^*$ , which is the onset glass transition temperature measured at a heating rate  $0.0167 \text{ Ks}^{-1}$  in the DSC. The VFT fits are plotted as lines in Fig. 2. The binary alloy is the most fragile of these liquids whereas the quaternary alloys are the strongest. Figure 3 shows a larger portion of the fragility plot that includes  $\text{SiO}_2$ , which is one of the strongest glass formers, and o-terphenyl, which is one of the most fragile glass formers. Figure 3 reveals that the Nb-Ni based alloys fit intermediate between the o-terphenyl and  $\text{SiO}_2$  in the fragility plot, with strong liquid behavior increasing as the number of components in the alloy increases.

For these Nb-Ni based alloys,  $D^*$  monotonically increases as the number of components in the alloy increases. This relationship is shown in Fig. 4. Extrapolation of the trend shown in Fig. 4 down to a one component system yields  $D^* \approx 2$ , which is in good agreement with the estimated fragility of pure metals using their melt viscosity and apparent activation energies for flow. Also in Fig. 4, the fragility parameters of the Nb-Ni based alloys are compared with the fragility parameters of other metallic glass forming alloys. The increase of the fragility parameter with increasing complexity of the system is also observed in Zr – based alloys. It reflects the slowdown in kinetics and thus the increase in glass forming ability in the alloys. This effect might be due to the size mismatch between the atoms in the alloy [10]. The fragilities for the two quaternary alloys are different and this suggests that the type of elements in an alloy also affects its fragility.

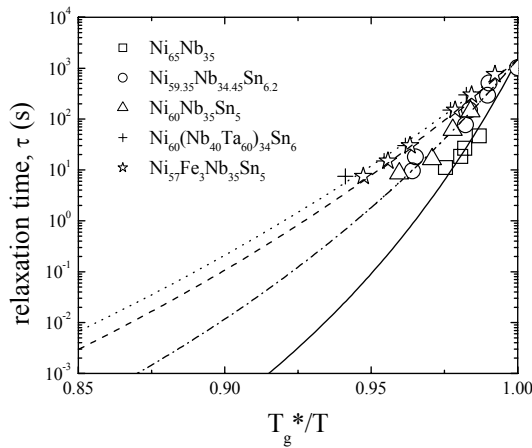


**Figure 2:** Fragility plot comparing the fragilities of the five Nb-Ni based alloys.  $\text{Ni}_{57}\text{Fe}_3\text{Nb}_{35}\text{Sn}_5$  alloy exhibits the strongest liquid behavior and the  $\text{Ni}_{65}\text{Nb}_{35}$  alloy exhibits the most fragile liquid behavior.

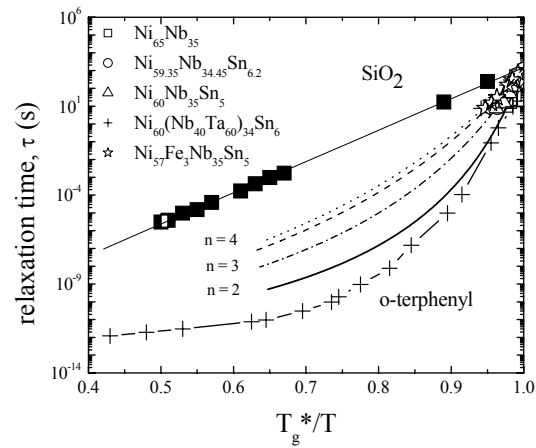


**Figure 3:** Fragility plot placing the Nb-Ni based alloys in the context of other glass forming materials by comparing their fragilities with that of o-terphenyl (most fragile glass former) and  $\text{SiO}_2$  (strongest glass former).

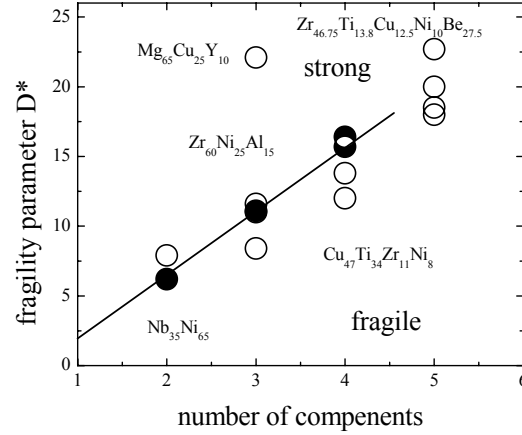


**Figure 4:** Fragility parameter,  $D^*$ , is plotted versus the number of components in the alloy. In this plot alloys of the Nb-Ni system (●) are compared to alloys of other systems (○).  $D^*$  of the alloy increases as the complexity of the alloy increases.

In a parallel study on the fragility of the  $Zr_{55-x}Ti_x(CuNi)_{18.25+y}Be_{26.25-y}$  (Vit1 series) system as the composition varies between  $9.62 \leq x \leq 16.5$  and  $0 \leq y \leq 6.25$ , it was found that  $D^*$  increases with increasing concentration of Ti and Cu and decreasing concentration of Zr and Be. Figures 5 and 6 show  $D^*$  for various compositions of Ti and Be. The results for Zr and Cu are analogous. When the fragility study of the Nb-Ni based and the Vit1 series alloys are considered together, they suggest that a balance between the size mismatch development by addition of components to a system and the concentration of those components can be reached to form a dense liquid with high  $D^*$  and therefore slow diffusivity.

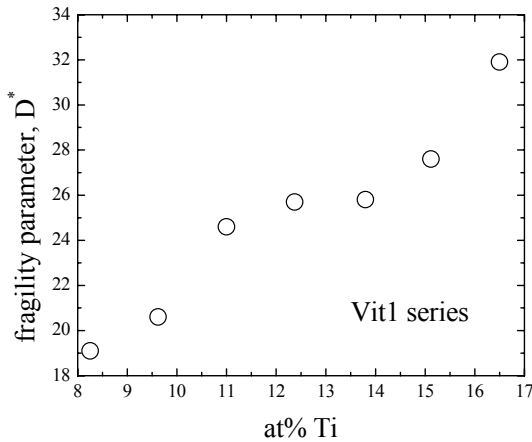


**Figure 5:** Fragility parameter,  $D^*$ , plotted versus atomic percent Titanium.  $D^*$  decreases for increasing Titanium concentration.

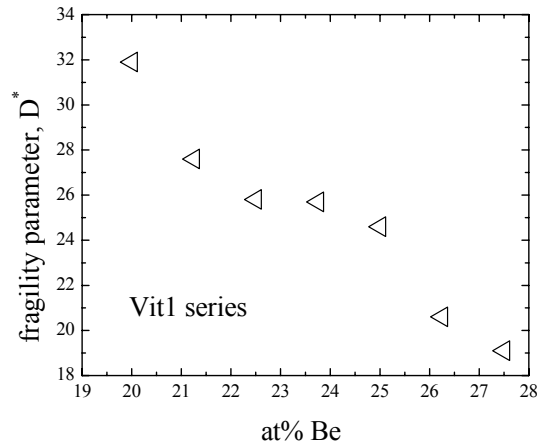


**Figure 6:** Fragility parameter,  $D^*$ , plotted versus atomic percent Beryllium.  $D^*$  decreases for increasing Beryllium concentration.

## CONCLUSIONS

The heating rate dependencies of the glass transition region and the crystallization temperature of the  $\text{Ni}_{65}\text{Nb}_{35}$ ,  $\text{Ni}_{60}\text{Nb}_{35}\text{Sn}_5$ ,  $\text{Ni}_{59.35}\text{Nb}_{34.45}\text{Sn}_{6.2}$ ,  $\text{Ni}_{60}(\text{Nb}_{40}\text{Ta}_{60})_{34}\text{Sn}_6$ , and  $\text{Ni}_{57}\text{Fe}_3\text{Nb}_{35}\text{Sn}_5$  metallic glasses were investigated with differential scanning calorimetry. The fragilities of the alloys were characterized with the fragility parameter  $D^*$ , and the VFT temperature,  $T_0$ . It was found that  $D^*$  increased monotonically with the number of components for the Nb-Ni based metallic glass forming alloys, which was very similar to a trend found for Zr- based alloys. In particular it was found that the structural stability of  $\text{Ni}_{65}\text{Nb}_{35}$  with respect to temperature change is improved by the addition of Sn. Furthermore it was found that the structural stability of the Nb-Ni-Sn alloys with respect to temperature change is improved with the addition of either Fe or Ta.

## ACKNOWLEDGEMENTS

The authors thank Haein Choi Yim for providing the samples and W. L. Johnson for fruitful discussions. This work was supported by DARPA (Grant no. DAAD-19-01-1-0525).

## REFERENCES

- [1] A. Inoue, T. Zhang, and T. Masumoto, Mater. Trans., JIM **31**, 425 (1991).
- [2] X. H. Lin and W. L. Johnson, J. Appl. Phys., **78** 6514 (1995).
- [3] A. Peker and W. L. Johnson, Appl. Phys. Lett., **63**, 2342 (1993).
- [4] T. Zhang, A. Inoue, and T. Masumoto, Mater. Trans., JIM **32**, 1005 (1991).
- [5] C. A. Angell, Science **267**, 1924 (1995).
- [6] T. A. Waniuk, R. Busch, A. Mashur, and W. L. Johnson, Acta Mater. **46**, 5229, (1998).
- [7] R. Busch, E. Bakke, and W. L. Johnson, Acta Metal., **46**, 4725 (1998).
- [8] R. Busch, W. Liu, and W.L. Johnson, J. Appl. Phys., **83**, 4134 (1998).
- [9] S. V. Nemilov, Glass Phys. Chem. **21**, 91, (1995).
- [10] X. P. Tang, U. Geyer, R. Busch, W. L. Johnson, and Y. Wu, Nature **402**, 160 (1999)